An Improved Measurement of Electron Antineutrino Disappearance at Daya Bay

David M. Webber, on behalf of the Daya Bay Collaboration

University of Wisconsin, Madison

Abstract

The theory of neutrino oscillations explains changes in neutrino flavor, count rates, and spectra from solar, atmospheric, accelerator, and reactor neutrinos. These oscillations are characterized by three mixing angles and two mass-squared differences. The solar mixing angle, θ_{12}, and the atmospheric mixing angle, θ_{23}, have been well measured, but until recently the neutrino mixing angle θ_{13} was not well known. The Daya Bay experiment, located northeast of Hong Kong at the Guangdong Nuclear Power Complex in China, has made a precise measurement of electron antineutrino disappearance using six functionally-identical Gadolinium-doped liquid scintillator-based detectors at three sites with distances between 364 and 1900 meters from six reactor cores. This proceedings describes the Daya Bay updated result, using 127 days of data collected between December 24, 2011 and May 11, 2012. The ratio of observed to expected events at the far site, under a null oscillation hypothesis, is $0.944 \pm 0.007(\text{stat}) \pm 0.003(\text{syst})$. A fit for θ_{13} in the three-neutrino framework yields $\sin^2 2\theta_{13} = 0.089 \pm 0.010(\text{stat}) \pm 0.005(\text{syst})$.

Keywords: Neutrino oscillation, Neutrino mixing, Reactor, Daya Bay

1. Introduction

In the Standard Model of particle physics, the three neutrino flavors ν_e, ν_μ, ν_τ, corresponding to the three generations of matter, are massless. However, the discovery of neutrino flavor oscillation [1, 2] has shown that neutrinos must have mass. Neutrinos propagate in definite mass eigenstates, denoted ν_1, ν_2, ν_3, and the mixing between the mass and flavor eigenstates is described by three mixing angles and one complex phase. Until this year, the smallest mixing angle, θ_{13}, was not known. Previous experiments observing reactor antineutrinos showed that $\sin^2 2\theta_{13} < 0.17$ at 90% confidence [3, 4]. More recently, beam neutrino [5, 6] and reactor antineutrino [7] experiments showed hints that $\sin^2 2\theta_{13}$ is nonzero with significances between 1 and 2.5 σ. In March 2012, the Daya Bay experiment released results showing that $\sin^2 2\theta_{13}$ is nonzero to better than 5σ [8], and this result was confirmed by the RENO experiment [9].

After this announcement, the Daya Bay experiment has updated its result including an additional 77 days (2.5×) exposure [10]. This proceedings describes an overview of neutrino oscillation and the Daya Bay experiment, and presents the updated result.

2. Neutrino Oscillation

As an introduction to neutrino oscillations, consider the simple case of two neutrinos, with flavor eigenstates ν_a and ν_b and mass eigenstates ν_1 and ν_2, related by one mixing angle θ.

$$\begin{pmatrix} \nu_a \\ \nu_b \end{pmatrix} = \begin{pmatrix} \cos\theta & \sin\theta \\ -\sin\theta & \cos\theta \end{pmatrix} \begin{pmatrix} \nu_1 \\ \nu_2 \end{pmatrix} \quad (1)$$

Neutrinos initially in a pure ν_a state will oscillate in and out of a pure ν_a state following the wave function

$$\Psi_{\nu_a}(x,t) = f(x,t) \sum_i U_{ai} e^{-i(m_i t/2E)}. \quad (2)$$

The "survival probability" for a neutrino initially in a pure ν_a state to remain in the ν_a state is

$$P(\nu_a \rightarrow \nu_a) = 1 - \sin^2(2\theta)\sin^2\left[1.27\Delta m_{21}^2 \frac{L}{E_\nu}\right], \quad (3)$$

Table 1: Reactor Uncertainties. Note that for a relative near-far measurement, only the uncorrelated uncertainties contribute.

Correlated		Uncorrelated	
Energy/fission	0.2%	Power	0.5%
IBD/fission	3%	Fission fraction	0.6%
		Spend fuel	0.3%
Combined	3%	Combined	0.8%

where θ governs the amplitude of the oscillation, $\Delta m^2_{21}(eV^2) = m^2_2 - m^2_1$ governs the frequency of oscillation, L (km) is the propagation distance, and E_ν (GeV) is the neutrino energy.

By extending this framework to three neutrinos [11] and making the approximation $\Delta m^2_{32} \approx \Delta m^2_{31} \approx \Delta m^2_{atm}$, one can write the survival probability of electron antineutrinos as

$$P_{\text{sur}} \approx 1 - \sin^2 2\theta_{13} \sin^2 \left(\Delta m^2_{32} \frac{L}{4E} \right) - \sin^2 2\theta_{12} \cos^4 2\theta_{13} \sin^2 \left(\Delta m^2_{21} \frac{L}{4E} \right). \quad (4)$$

From equation 4, it is clear that two terms dominate the survival probability. For a fixed antineutrino energy range, the first term contains the larger Δm^2_{32} and becomes dominant at smaller baselines. The second term depends on the smaller Δm^2_{21} and applies to the measurement of θ_{12} at larger baselines. The latter measurement was performed by KamLAND [12], and the former is well suited to a $\approx 2km$ baseline reactor antineutrino experiment.

3. The Daya Bay Experiment

The Daya Bay experiment takes place at the Daya Bay nuclear power complex near Shenzhen, China. There are 6 reactors spaced in pairs along the coast in three nuclear power plants. Each reactor is capable of producing 2.9 GW thermal power, for a total site power of 17.4 GW_{th}. The reactor companies provide time-averaged information about the reactor power and the isotope fractions to the experiment; uncertainties on these quantities is given in table 1. Overall, the nuclear power complex produces 3×10^{21} antineutrinos per second. During the collection of this dataset, there were 6 detectors in installed in three experimental halls, as shown in figure 1. The detectors are installed underground with baselines and overburdens summarized in table 2.
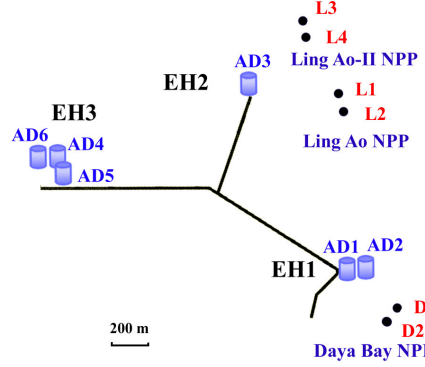

Figure 1: The layout of the Daya Bay experiment. The six reactors (D1,D2,L1,L2,L3,L4) are located at the Daya Bay, Ling Ao, and Ling Ao-II nuclear power plants. The Daya Bay antineutrino detectors (ADs) are located underground in three experimental halls (EHs). Underground tunnels connect the three sites and provide access from the surface.

Table 2: Experimental hall overburden (m.w.e.) and approximate baselines to reactor cores (m).

	Overburden	D.B.	L.A.	L.A.II
EH1	280	360	860	1310
EH2	300	1250	480	530
EH3	880	1910	1540	1550

The Daya Bay antineutrino detectors (ADs) have 3 cylindrical nested fluid volumes separated by two acrylic vessels. The innermost volume holds 20T of linear-alkyl-benzene-based liquid scintillator, doped with 0.1% Gadolinium. This fluid optimizes the detection of the the inverse beta decay (IBD) process $\bar{\nu}_e + p \rightarrow n + e^+$, where the positron carries most of the neutrino energy and is tagged by neutron capture on Gadolinium. The intermediate volume contains undoped liquid scintillator (LS) and serves as a gamma-ray catcher for light escaping from the central volume. The outer volume contains a non-scintillating mineral oil (MO) buffer. Scintillation light is collected by reflectors on the top and bottom of the detector and by 192 photomultiplier tubes on the walls of the AD.

The detectors are constructed on the surface in a clean environment, and then transported underground for filling. The detector is filled simultaneously from three fluid reservoirs to keep the fluid levels equal and to minimize the stress on the acrylic vessels. After filling, the detectors are transported to one of the three experimental halls, where they are placed in a water pool. Each water pool is filled with ultra-pure (15 MOhm)

water and serves the dual function of radiation shield and active muon veto. The water pool is covered with a light-tight cover and an array of resistive-plate chambers (RPCs) [13] is rolled over the top as an additional cosmic ray veto. A schematic of an AD installed in the water pool is shown in figure 2. The detectors are functionally identical and have excellent consistency, as studied in a side-by-side comparison of the first two detectors in hall 1 [14].
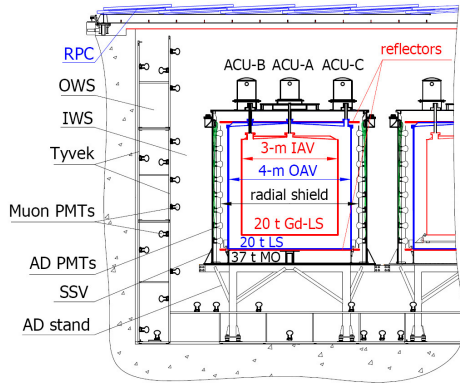

Figure 2: Schematic of installed antineutrino detector (AD). The AD has three cylindral nested fluid volumes, filled with gadolinium-doped liquid scintillator, undoped liquid scintillator, and mineral oil. Top and bottom reflectors guide scintillation light into 192 8-inch photomultiplier tubes (PMTs) on the walls of the detector. The ADs are installed on supports in a water pool instrumented with PMTs. The water pool and the RPCs serve as a cosmic ray veto. Automated calibration units (ACUs) periodically lower sources into the detector for calibration.

4. Event Selection

Although care is taken to keep radioactive materials out of the detectors, antineutrino interactions in the detector are rare compared to ambient radioactive backgrounds. With a trigger threshold of 0.4 MeV, the single-event rate is $\approx 250 Hz (\approx 140 Hz)$, whereas the neutrino interaction rate is $\approx 650/day (\approx 75/day)$ at the near (far) sites. The Daya Bay analysis uses coincident events to reduce this background. Specifically, the detectors are optimized for observing the inverse beta decay (IBD) process $\bar{\nu}_e + p \rightarrow n + e^+$. The positron carries most of the energy of the neutrino, and it thermalizes and annihilates quickly. The average neutron capture time in GdLS is 28μs. This neutron capture provides a delayed signal which tags the prompt events. After rejecting flashing PMT events and applying a muon veto, IBD candidates are selected from all prompt-delayed coincidence events which have

- Prompt energy between 0.7 and 12 MeV

- Delayed energy between 6 and 12 MeV

- Time between prompt and delayed events between 1 and 200 μs

- No other signals $400\mu s$ before or $200\mu s$ after the delayed neutron event.

The efficiency and uncertainty of these cuts, as well as other detector-related uncertainties, is summarized in table 4.

5. Backgrounds

Despite the resolving power of the coincidence IBD selection, several backgrounds still contribute to the IBD candidates. First, independent single events can occur with small time-separation, giving an accidental coincidence. These events are statistically subtracted by calculating the expected rate of accidentals using the rate of prompt-like single events, delayed-like single events, and the coincidence interval.

Second, a fast cosmogenic neutron can mimic an IBD signal by first scattering inside the detector to give prompt light and then capturing on Gd to give a delayed signal. Since the neutron energy deposition is expected to be flat below 50 MeV, these neutron events can be subtracted from the IBD candidates by considering the prompt-like signal energies with 12-50 MeV and extrapolating into the IBD signal region 0.7-12 MeV. This method is validated by examining fast-neutron events tagged with a muon.

Third, long-lived cosmogenic isotopes can create an IBD-like coincidence. For example, $^9Li \rightarrow ^9Be + e^- + \bar{\nu}_e$ with half-life 178ms, followed by $^9Be \rightarrow n + 2\alpha$ yields prompt light from the electron and a delayed neutron capture. This background is studied vs. time after a muon and controlled to $\approx 0.2\%$ of the IBD signal.

Fourth, the 0.5-Hz $^{241}Am - ^{13}C$ neutron sources introduce a background when they are retracted into the automated calibration units on the top of the AD. The neutron scatters off of iron, then captures on stainless steel, producing correlated prompt and delayed signals corresponding to $0.3 \pm 0.3\%$ of the IBD rate at the far site.

Other backgrounds result from alpha and neutron interactions with carbon and iron in the detector materials. Although the uncertainties on these contributions are high, these are negligible effects overall. A summary of the background contributions is given in table 3.

Table 3: Summary of Data Set. Efficiencies are dominated by the muon veto rates, which vary with the overburden at each site. Backgrounds are subtracted from the IBD candidates to yield the IBD rate per day.

	Near Sites			Far Site		
	EH1		EH2	EH3		
	AD1	AD2	AD3	AD4	AD5	AD6
IBD Candidates	69121	69714	66473	9788	9669	9452
DAQ livetime	127.5470		127.3763	126.2646		
Efficiency	0.8015	0.7986	0.8364	0.9555	0.9552	0.9547
Accidentals (/day)	9.73±0.10	9.61±1.10	7.55±0.08	3.05±0.04	3.04±0.04	2.93±0.03
Fast neutrons (/day)	0.77±0.24		0.58±0.33	0.05±0.02		
^{8}He/^{9}Li (/AD/day)	2.9±1.5		2.0±1.1	0.22±0.12		
AmC (/AD/day)	0.2 ± 0.2					
^{13}C(α,n)^{16}O (/AD/day)	0.08±0.04	0.07±0.04	0.05±0.03	0.04±0.02	0.04±0.02	0.04±0.02
Antineutrino Rate (/day)	662.47±3.00	670.87±3.01	613.53±2.69	77.57±0.85	76.62±0.85	74.97±0.84

Table 4: Detector Uncertainties. The spill-in efficiency is larger than 100% since more IBD neutrons drift inward into the central GdLS target volume than outward into the LS volume. For a relative near-far measurement, only the uncorrelated uncertainties contribute.

	Efficiency	Correlated	Uncorrelated
Target Protons		0.47%	0.03%
Flasher Cut	99.98%	0.01%	0.01%
Delayed Energy Cut	90.9%	0.6%	0.12%
Prompt Energy Cut	99.88%	0.10%	0.01%
Multiplicity Cut		0.02%	< 0.01%
Capture Time Cut	98.6%	0.12%	0.01%
Gd Capture Ratio	83.8%	0.8%	< 0.1%
Spill-in	105.0%	1.5%	0.02%
Livetime	100.0%	0.002%	< 0.01%
Combined	78.8%	1.9%	0.2%

6. Results

Overall, the Daya Bay experiment collected over 230,000 IBD candidates during the running period from December 24, 2011 to May 11, 2012. The dataset and backgrounds are summarized in table 3, and the detector uncertainties are summarized in table 4. The antineutrino rates are consistent within each experimental hall, and the dominant uncorrelated detector systematic uncertainty is the delayed energy cut at 6 MeV.

The event rates at the near sites are weighted by reactor power and baseline to predict the event rate at the far site under a null-oscillation hypothesis. The ratio of far to near events is

$$R = 0.944 \pm 0.007(\text{stat}) \pm 0.003(\text{syst}). \quad (5)$$

The event rate vs. day at the three experimental sites tracks the reactor power, and a clear deficit is visible for the far site (Fig. 3).
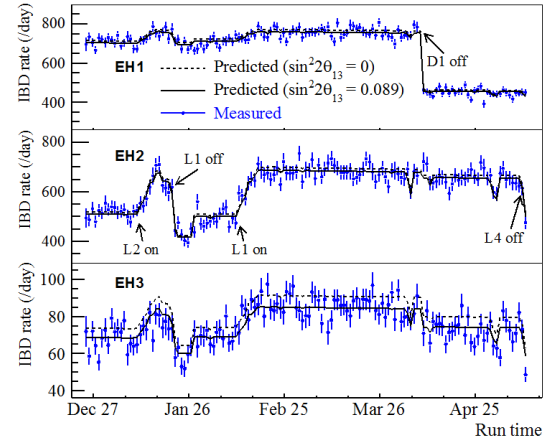

Figure 3: The measured neutrino events (points) are in good agreement with the prediction from reactor power (lines) for $\sin^2 2\theta_{13} = 0.089$. At the far site (EH3), the null oscillation hypothesis clearly disagrees with the data.

A relative rate-only analysis was performed on the IBD rates in the 6 detectors, independent of any reactor flux model. In the standard 3-neutrino framework, a fit for θ_{13} yields $\sin^2 2\theta_{13} = 0.089 \pm 0.010(\text{stat}) \pm 0.005(\text{syst})$ (Fig. 4). A superposition of the predicted and observed neutrino events with energy, overlaid with the rate-only best-fit line, is shown in figure 5.

7. Future

During the summer of 2012, the Daya Bay experiment will install the final two antineutrino detectors. A
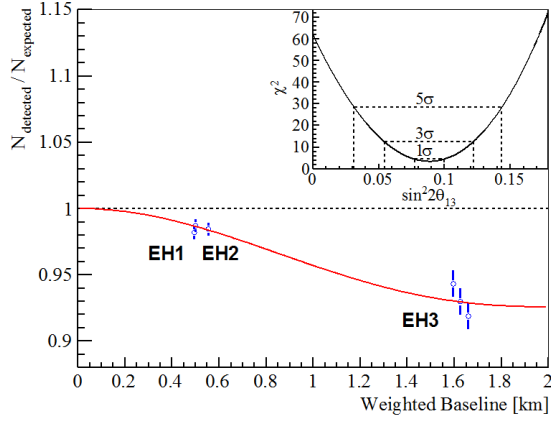
Figure 4: The ratio of predicted to observed events at the six detectors vs. flux-weighted baseline is fit for $\sin^2 2\theta_{13}$. The χ^2 plot in the upper right shows $\sin^2 2\theta_{13} = 0$ is excluded by over 5σ.
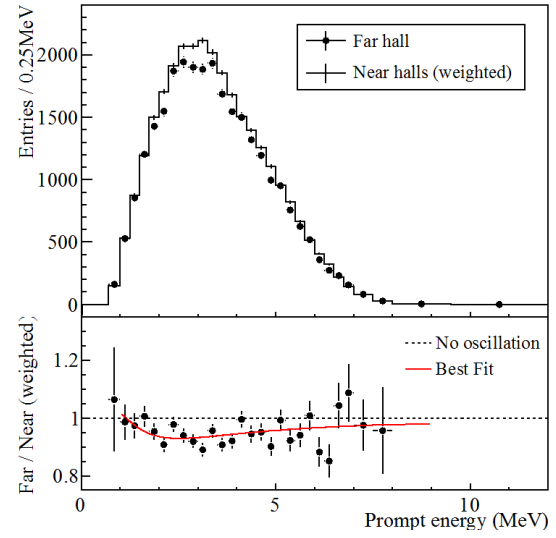

Figure 5: The upper plot shows the prompt energy spectrum at the near and far experimental halls, weighted by the reactor power and baseline. The lower plot shows the ratio, with the best-fit rate-only analysis curve superimposed.

series of special calibration measurements will be made using radioactive sources deployed along strings from the top of the detector and on an arm inserted into the central volume of one detector. These measurements will improve the understanding of detector uniformity and energy resolution.

Continuing its science mission over the next 2-3 years, Daya Bay will make a definitive and precise measurement of $\sin^2 2\theta_{13}$. In addition, the location of the oscillation maximum in the positron energy spectrum will allow a measurement of Δm_{ee}^2, a combination of Δm_{31}^2 and Δm_{32}^2.

In addition, Daya Bay will pursue several secondary scientific and technical studies. With the largest antineutrino dataset ever collected, Daya Bay will make the best reactor antineutrino flux and spectra measurements. Daya Bay will also measure the rates of cosmogenic neutron and isotope production at a range of modest depths and energies. In terms of technical studies, Daya Bay will demonstrate the multi-year operation of functionally identical detectors and measure long-term GdLS stability. Finally, the Day Experiment has the potential to search for non-standard neutrino interactions [15]. Although Daya Bay has produced the most precise value of $\sin^2 2\theta_{13}$ to date, there are many more results still to come.

8. Acknowledgements

References

[1] Y. Fukuda *et al.* (Super-Kamiokande Collaboration), Evidence for oscillation of atmospheric neutrinos, Phys. Rev. Lett. 81 (1998) 1562–1567.

[2] Q. R. Ahmad *et al.* (SNO Collaboration), Direct evidence for neutrino flavor transformation from neutral-current interactions in the sudbury neutrino observatory, Phys. Rev. Lett. 89 (2002) 011301.

[3] M. Apollonio *et al.* (CHOOZ Collaboration), Limits on neutrino oscillations from the CHOOZ experiment, Phys.Lett. B466 (1999) 415–430. arXiv:hep-ex/9907037.

[4] M. Apollonio *et al.* (CHOOZ Collaboration), Search for neutrino oscillations on a long baseline at the CHOOZ nuclear power station, Eur.Phys.J. C27 (2003) 331–374. arXiv:hep-ex/0301017.

[5] P. Adamson *et al.* (MINOS Collaboration), Improved search for muon-neutrino to electron-neutrino oscillations in MINOS, Phys.Rev.Lett. 107 (2011) 181802. arXiv:1108.0015.

[6] K. Abe *et al.* (T2K Collaboration), Indication of Electron Neutrino Appearance from an Accelerator-produced Off-axis Muon Neutrino Beam, Phys.Rev.Lett. 107 (2011) 041801. arXiv:1106.2822.

[7] Y. Abe *et al.* (Double-Chooz Collaboration), Indication for the disappearance of reactor electron antineutrinos in the Double Chooz experiment, Phys.Rev.Lett. 108 (2012) 131801. arXiv:1112.6353.

[8] F. P. An *et al.* (Daya Bay Collaboration), Observation of electron-antineutrino disappearance at daya bay, Phys. Rev. Lett. 108 (2012) 171803.

[9] J. K. Ahn *et al.* (RENO Collaboration), Observation of Reactor Electron Antineutrinos Disappearance in the RENO Experiment, Physical Review Letters 108 (19) (2012) 191802. arXiv:1204.0626.

[10] F. P. An *et al.* (Daya Bay Collaboration), Improved measurement of electron anti-neutrino disappearance at daya bay, in preparation.

[11] Z. Maki, M. Nakagawa, S. Sakata, Remarks on the unified model of elementary particles, Prog.Theor.Phys. 28 (1962) 870–880.

[12] Abe, S. *et al.* (KamLAND Collaboration), Precision measurement of neutrino oscillation parameters with kamland, Phys. Rev. Lett. 100 (2008) 221803.

[13] J. Xu, M. Guan, C. Yang, Y. Wang, J. Zhang, C. Lu, K. McDonald, R. Hackenburg, K. Lau, L. Lebanowski, et al., Design and preliminary test results of daya bay rpc modules, Chinese Physics C 35 (2011) 844.

[14] F. P. An *et al.* (Daya Bay Collaboration), A side-by-side comparison of daya bay antineutrino detectors, Nuclear Instruments and Methods in Physics Research Section A: Accelerators, Spectrometers, Detectors and Associated Equipment 685 (0) (2012) 78 – 97.

[15] D. Dwyer, K. Heeger, B. Littlejohn, P. Vogel, Search for Sterile Neutrinos with a Radioactive Source at Daya Bay arXiv:1109.6036.